

Theoretical Computational of Electronic and Transport Properties and Optical Conductivity of Monolayer NiS₂ under Mechanical Strain

Nguyen Hoang Linh¹, Tran The Quang^{2*}, Nguyen Minh Son¹,
To Toan Thang¹, Vuong Van Thanh¹, Do Van Truong¹

¹Hanoi University of Science and Technology, Ha Noi, Vietnam

²Thai Binh University, Thai Binh, Vietnam

*Corresponding author email: tranthequang12@gmail.com

Abstract

In this study, the first-principle calculations using Density Functional Theory are used to evaluate the mechanical, electronic and transport properties of the NiS₂ monolayer structure. The obtained results show that the monolayer structure NiS₂ is broken at the tensile strain of 18% in the x direction and 14% in the y direction. The ultimate strengths are 8.0 N/m and 6.45 N/m in the x and y directions, respectively. At the ground state, the band gap is 0.49 eV with the conduction-band minimum (CBM) at the K'-Γ path and the valence-band maximum (VBM) at the Γ point. Under the strain, the energy band structure is changed and tends to become a metallic material. In addition, the effective mass, which is an important parameter related to the charged particle transportability, is also investigated. The effective mass of the electron decreases while that of the hole increases. The carrier mobility of the electron confirmed is more enhanced than that of the hole. Besides, the optical conductivity properties of NiS₂ structure confirmed are pretty good. The obtained results indicate the potential of using the mechanical strain to control the electronic, optical conductivity and transport properties of the NiS₂ monolayer structure in microelectromechanical and optoelectronic devices.

Keywords: 2D materials, optical conductivity, DFT calculations, electronic structures, transport properties.

1. Introduction

Recently, studies of low-dimensional (2D) materials have revealed their potential applications in field-effect transistors (FETs), optical sensors and other electronic devices [1]. The remarkable advantages of this material group that we can mention include their small size, lightweight nature, and particularly their outstanding physical and mechanical properties in comparison to bulk materials. This may be one of the main reasons explaining why numerous 2D materials such as pentagon, hexagonal chalcogenides, dichalcogenides, and borophene have been newly discovered [2-4].

The NiS₂ monolayer has sandwich structures that have been involved in several practical applications such as semiconductor and nanoelectronic devices [5]. In a previous study, Wenqi Xiong *et al* [6] demonstrated that the monolayer NiS₂ is a semiconductor material and possesses high stability in the equilibrium state. Besides, the study has shown that this material has high flexibility with low elastic modulus, high anisotropic electronic properties, and excellent optical properties that support hydrogen production in the water-splitting application. However, this study only investigates the mechanical, electronic, and optical properties at equilibrium.

H.Khalatbari *et al.* [5] have used the substituting atom method in order to modify the energy band structure of the monolayer NiS₂ material. The disadvantage of the method is that it is difficult to accurately determine the structure and position of the doped atoms in practice. Hongye Yang *et al.* [7] have demonstrated that monolayer NiS₂ can convert semiconductor properties from direct to indirect semiconductors under the biaxial tensile strain. Although there have been many studies on the mechanical properties, electronic properties, and optical properties of 2D materials [2, 3], the studies on those properties of NiS₂ monolayer materials are still limited and unsystematic. Moreover, recently, the research direction of using mechanical strain to control the electronic and optical properties of materials has been attracting much attention from scientists [4, 8]. Therefore, studying the influence of mechanical strain on the electronic and optical properties of NiS₂ material is a necessary task in order to find outstanding properties for application in semiconductor and nanoelectronic devices.

In this study, by means of the first-principle calculations method, the research evaluates the mechanical parameters such as the elastic coefficient, the elastic modulus, the Poisson's ratio, and the critical strain corresponding to the ultimate strength of the monolayer NiS₂ material. In addition, the influences of

the mechanical strain in the x and the y directions on the energy band structures, particle transportability and carrier mobility of the monolayer NiS₂ material are clarified. Consequently, our results are trustworthy and fundamental for improving the service quality of nanoelectronic devices in the near future.

2. Methodology

The optimized structure and the electron-related computations of the NiS₂ monolayer were made by Quantum Espresso at 0K. Exchange-correlation (XC) energy was determined through the Perdew-Burke-Ernzerhof (PBE) functional by the generalized gradient approximation (GGA) method. We selected the wave functions with the threshold for kinetic energy and charge density of 60 Ry and 720 Ry, respectively. To avoid interaction between layers, a vacuum space of 30 Å was set [9]. The position of atoms was detected by the minimum relax energy Broyden-Fletcher-Goldfarb-Shanno (BFGS) with the total energy condition of 1×10^{-6} eV and the stress condition of 10^{-5} eV/Å. The Monkhorst-Pack method was applied to select the k -meshes of $15 \times 15 \times 1$ for the Brillouin zone.

3. Results and Discussion

3.1. Mechanical Properties

The equilibrium state of the NiS₂ monolayer is determined via the BFGS optimization algorithm. The lattice vectors of NiS₂ are $a = b = 3.33$ Å (Fig. 1), and these results match the previous research [5]. Besides, the parameters including the elastic constants C_{ij} , Young's modulus, and Poisson's ratio are calculated through the Thermo-pw code. The mechanical parameters are listed in Table. 1. Generally, the NiS₂ structure has quite small elastic coefficients, but it satisfies conditions of Born's criterion for mechanical stability, i.e $C_{11} > |C_{12}| > 0$ và $C_{66} > 0$ [10]. The elastic modulus of NiS₂ is smaller than a few previously studied 2D materials such as ZrS₂ (57.22 N/m), ZrSe₂ (52.33 N/m) [3].

Fig. 2 describes the stress-strain curve of NiS₂ in the x and y directions. The tensile strains on the lattice vector are calculated by $\varepsilon = (l_1 - l_0)/l_0$ where l_1 and l_0 are dimensions of the strained state and equilibrium state, respectively. We note that units are rescaled with a vacuum space because the NiS₂ structure is a single layer. Results show that the mechanically critical strain of NiS₂ structure in the x direction is higher than that in the y direction. The ultimate strength in the x direction is 8.0 N/m at $\varepsilon_{xx} = 18\%$. Under the tensile strain in the y direction, the structure is broken at $\varepsilon_{yy} = 14\%$ with a maximum value of 6.45 N/m. The ultimate strength of NiS₂ structure is greater than that of Germanene (6.0 N/m), and Stanene (4.1 N/m) [11].

Table. 1. Lattice parameters a , b (Å), thickness h (Å), elastic constant C_{ij} (N/m), elastic modulus E (N/m) and Poisson's ratio ν .

Monolayer	$a = b$	h	C_{11}	C_{22}	C_{12}	C_{66}	$E_{xx} = E_{yy}$	$\nu_{xx} = \nu_{yy}$
1T-NiS ₂	3.33	2.39	56.58	56.58	21.31	17.80	50.68	0.38

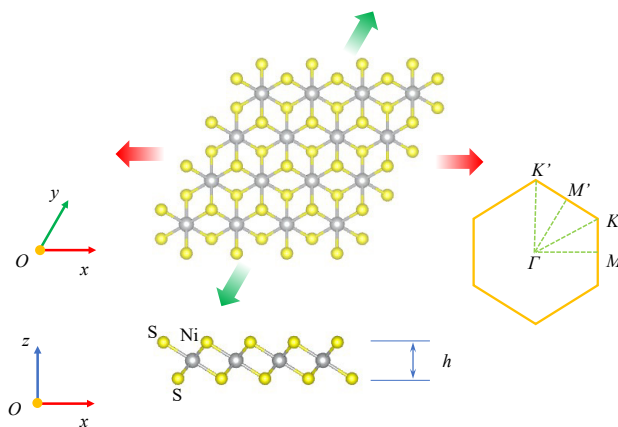


Fig. 1. The structure and Brillouin zone of NiS₂ monolayer with the high symmetry points

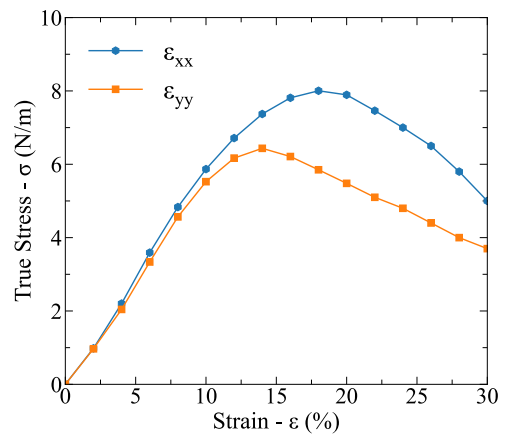
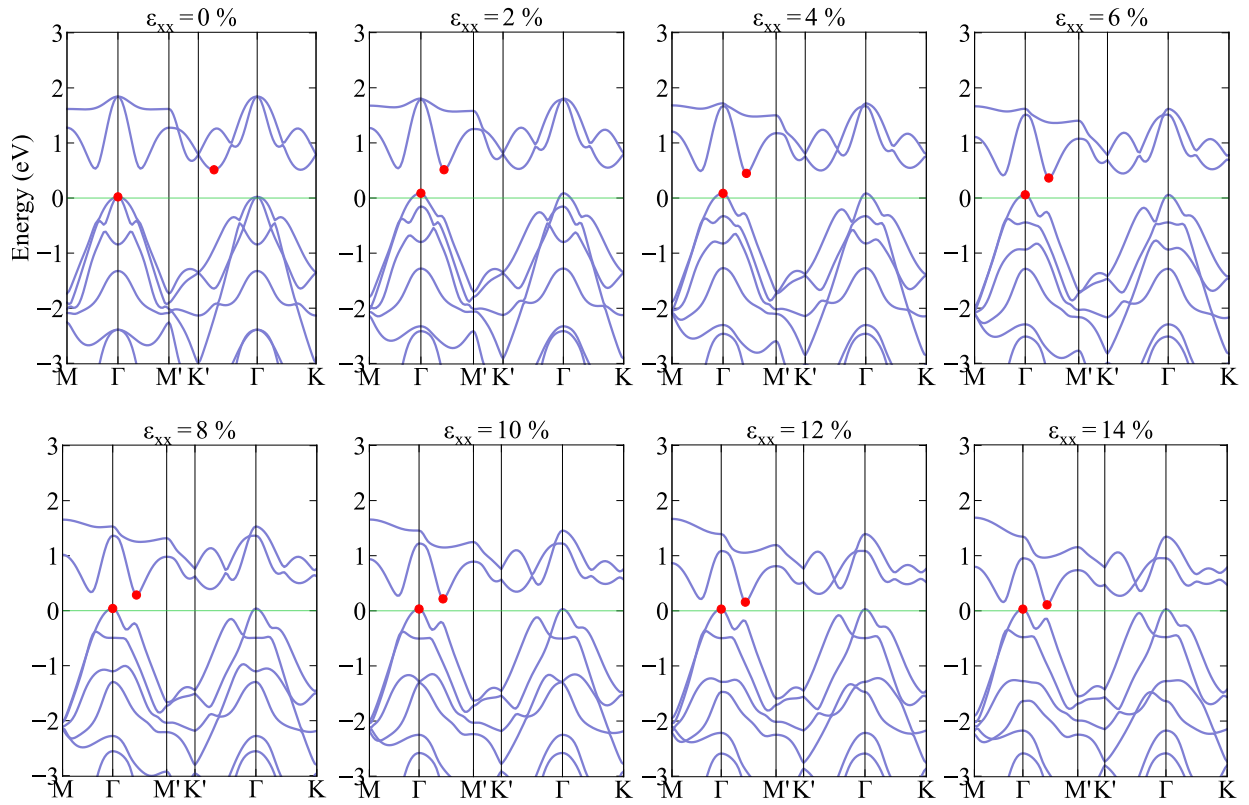
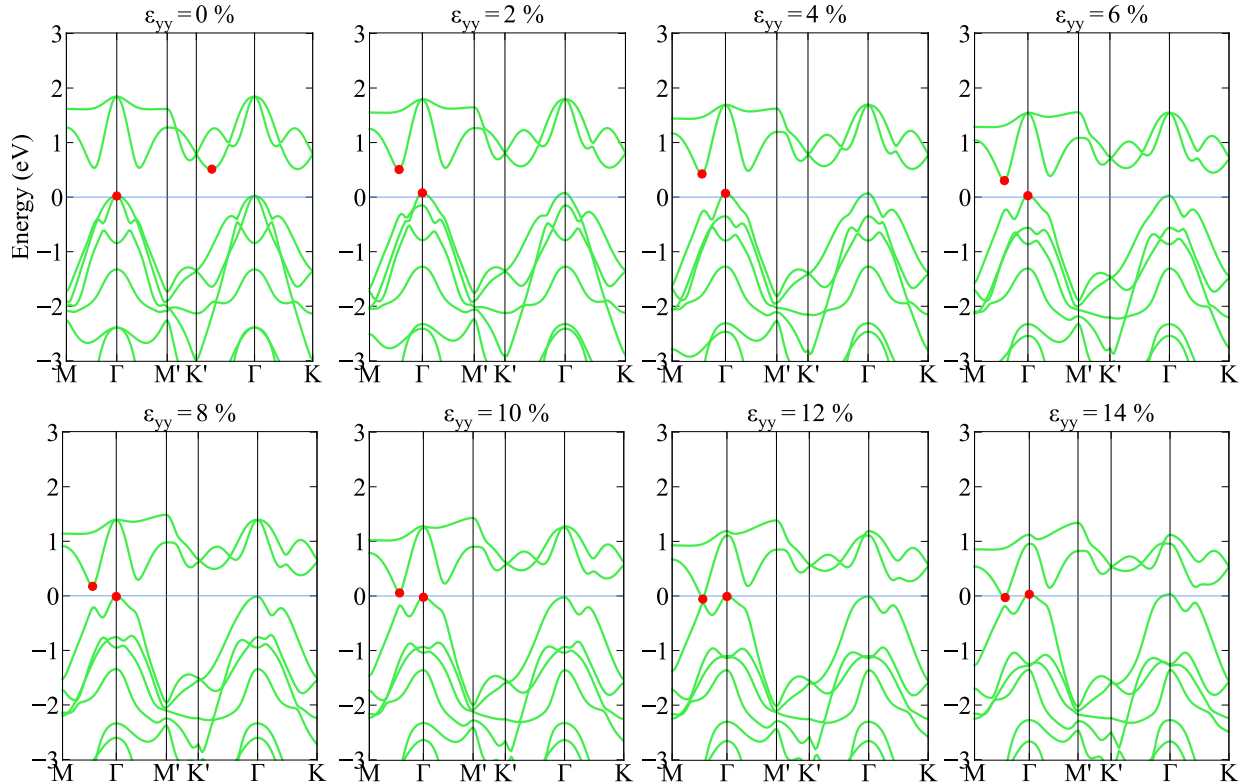


Fig. 2. The stress-strain curves of NiS₂ structure under tensile strain in the x and y directions



(a)



(b)

Fig. 3. Energy band structures of NiS2 monolayer under the tensile strain in (a) x and (b) y direction

3.2. Electronic Properties

In this study, we calculate the electronic band structures, which is an important parameter. Our results show that NiS₂ is a semiconductor, which is calculated by the PBE theory and the M-Γ-M'-K'-Γ-K path in the reciprocal zone. The band gap of NiS₂ determined is 0.49 eV with the conduction-band minimum (CBM) at the Γ point and the valence-band maximum at the K'-Γ zone. The results are consistent with that of the previous theoretical study [12].

In practice, the strain always appears undesirable in monolayer structures and can change their material properties. To clarify this issue, we investigate the effect of strain (up to 14%) on the energy band structures of the NiS₂ monolayer. Fig. 3 illustrates the effect of tensile strain in the *x*, and *y* directions on the band structure of the NiS₂ monolayer. The results show that the strain has a significant impact on the distributions of the VBM and CBM. Under the tensile strain in the *x* direction, the CBM tends to transfer from K'-Γ to Γ-M' path, while the VBM remains at the Γ point, as shown in Fig 3(a). Similarly, the distribution of the CBM only changes from K'-Γ to M-Γ path under the strain in the *y* direction, as shown in Fig 3 (b).

Fig. 4 depicts the effect of strain along the *x* and *y* directions on the band gap of the NiS₂ monolayer. The results show that the band gap decreases as a linear function under the tensile strain in the *xy*-plane. When straining in the *x* direction, the band gap is drastically decreased from 0.49 eV at $\epsilon_{xx} = 0\%$ to 0.08 eV (down ~84%) at $\epsilon_{xx} = 14\%$. In particular, at the tensile strain of 14% in the *y* direction, the NiS₂ structure exhibits metal properties with a band gap of 0 eV. Thus, we see that the strain is one of the main factors that can change the distribution of the electron bands, and can control the band gap of the structure.

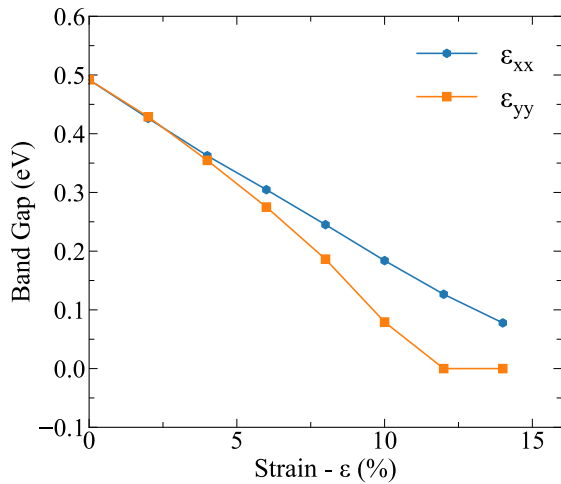


Fig. 4. Effect of strain along the *x* and *y* directions on the band gap of the NiS₂ monolayer

3.3. Transport Properties

To explore the effect of the strain on the transport properties of NiS₂ monolayer, the tensile strain is applied to investigate in the range of 0% to 14%. The μ_{2D} mobility characteristic for electron and hole transport is calculated based on the formula [13]:

$$\mu_{2D} = \frac{e\hbar^3 C_{2D}}{k_B T |m^*|^2 E_d^2} \quad (1)$$

here, *e* is the electron charge, \hbar is the Planck constant, *C*_{2D} is the elastic modulus of the crystal, *k*_B is the Boltzmann constant, *E*_d is the deformation potential constant, and *m*^{*} is the effective mass of the electron or hole. We calculate the deformation potential constants by equation (2) and changing the extremum peak *E*_{edge} in the energy band structures diagram. *M*^{*} roles as the mass of particles can be attained by fitting the parabolic function from the relationship between the total energy *E* and the wavevector *k* [13]:

$$E_d = \frac{E_{edge}}{\epsilon}; \quad \frac{1}{m^*} = \left| \hbar^2 \frac{\partial^2 E}{\partial k^2} \right| \quad (2)$$

The effective mass *m*^{*} is an important parameter that decides to carrier the mobility of charged particles. Fig. 5 illustrates the change of the effective mass *m*^{*} under the strain at 300K. The results show that carrier mobility is a function of the tensile strain. At the equilibrium ($\epsilon = 0\%$), the effective mass of electron (*m*_e) and hole (*m*_h) are 0.58 *m*₀ and 1.25 *m*₀, respectively. At the tensile strain of $\epsilon = 2\%$ in the *x* and *y* directions, *m*_e and *m*_h are suddenly changed from the equilibrium. *M*_e increases 70.36% in the *x* direction and 72.78% in the *y* direction, while *m*_h decreases 70.36% in the *x* direction and 72.78% in the *y* direction. This sudden change is caused by moving the position of the CBM point from the K'-Γ path to the Γ-M' path in the *x* direction and from the K'-Γ path to the M-Γ path in the *y* direction. *M*_h decreases as the strain increases. *M*_h is equal to 0.32 *m*₀ at the strain of 14% in the *x* direction and 0.31 *m*₀ in the *y* direction. *M*_e tends to decrease gradually by the strain from 2% to 14%. However, at the strain of 14%, *m*_e increases relative to the equilibrium, increasing by 13.34% in the *x* direction and 31% in the *y* direction. Besides, the results show the effective mass of the hole is always smaller than that of the electron at the strain from 2% to 14% in the *x* and *y* directions. The obtained results also confirm that the effective mass of the NiS₂ monolayer can be controlled by using the engineering strain. The results of the effect of the tensile strain on the carrier mobility (μ) are shown in Fig. 6.

Based on the found parameters listed in Table. 2, we have calculated the transport properties of the NiS₂ structure. In the equilibrium state ($\epsilon = 0\%$), the mobility of the hole (μ_h) is 156.0 cm²/Vs (in the *x* direction) and 268.7 cm²/Vs (in the *y* direction) while

the mobility of the electron (μ_e) is 217.7 cm^2/Vs (in the x direction) and 230.7 cm^2/Vs (in the y direction) at the room temperature conditions ($T=300\text{K}$). At the tensile strain $\varepsilon = 2\%$, because the CBM is moved from the $M - \Gamma$ path to the $\Gamma - M'$ path, μ_h suddenly increases up to 254.0 cm^2/Vs in the x direction and 476.5 cm^2/Vs in the y direction (~ 1.8 times higher than the equilibrium). In contrast, μ_e decreases sharply and reaches 75.0 cm^2/Vs in the x direction and 77.3 cm^2/Vs in the y direction (~ 3 times smaller than the equilibrium). From 2% to 14% of the tensile strain, the results show that both μ_e and μ_h tend to increase as the

strain increases. Under the strain in the x direction, μ_h increases rapidly and reaches 611.3 cm^2/Vs at $\varepsilon = 14\%$ (an increase of 29.2 % from equilibrium), and μ_e reaches 169.5 cm^2/Vs at $\varepsilon = 14\%$ (a decrease of 28.5% from equilibrium), as depicted in Fig. 6 (a). Similarly, under the strain in the y direction, at strain $\varepsilon = 14\%$, μ_h and μ_e reach 1108.3 cm^2/Vs (increasing $\sim 61.6\%$) and 134.4 cm^2/Vs . (decreasing $\sim 71.7\%$), as depicted in Fig. 6 (b). This issue is similar to MoS_2 structures, which were demonstrated by H. V. Phuc *et al* [14].

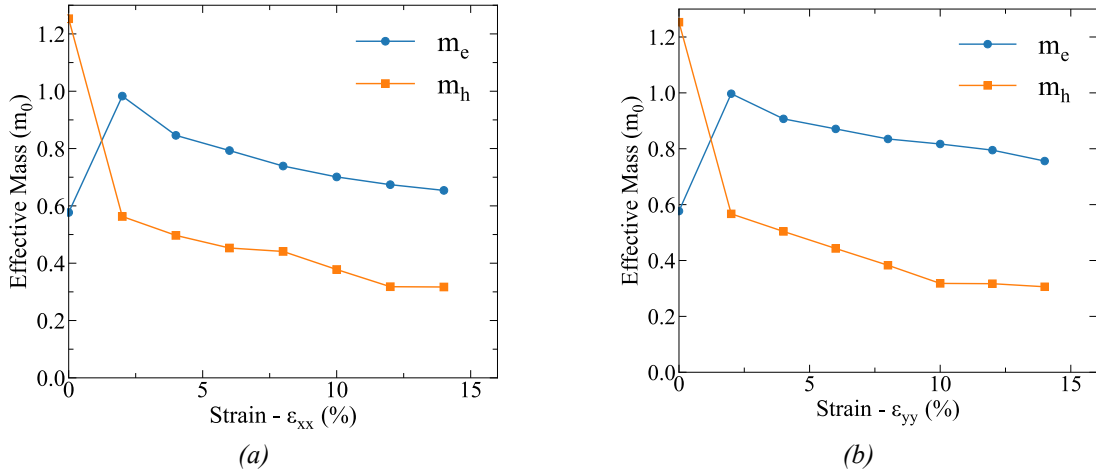


Fig. 5. Effective mass as a function of the tensile strain in (a) x and (b) y directions

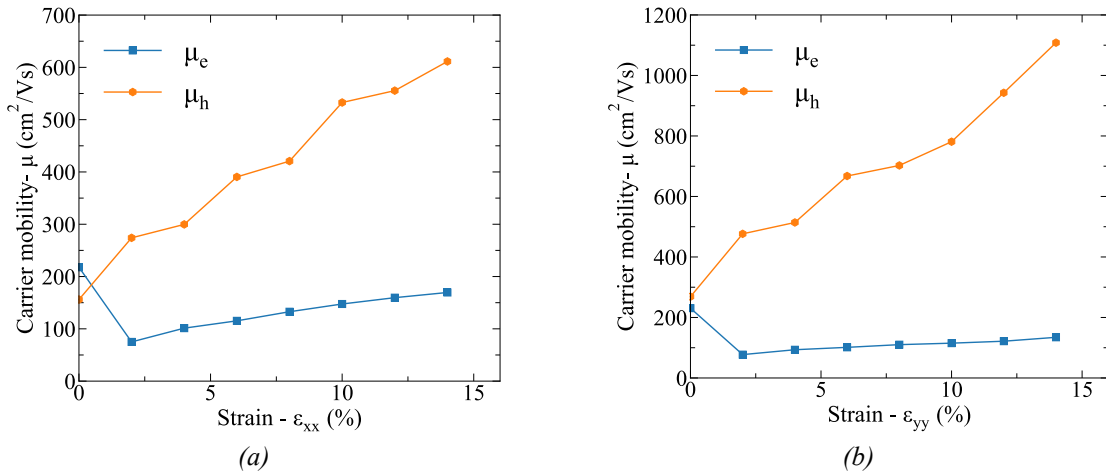


Fig. 6. The relationship between carrier mobility and the tensile strain

Table 2. Elastic modulus C_{2D} (N/m), effective mass m^* (m_0), deformation potential energy E (eV)

Elements	C_{2D} (N/m)	m^* (m_0)	E_d^x (eV)	E_d^y (eV)
Electron	50.68	0.38	3.86	3.75
Hole	50.68	0.38	2.10	1.60

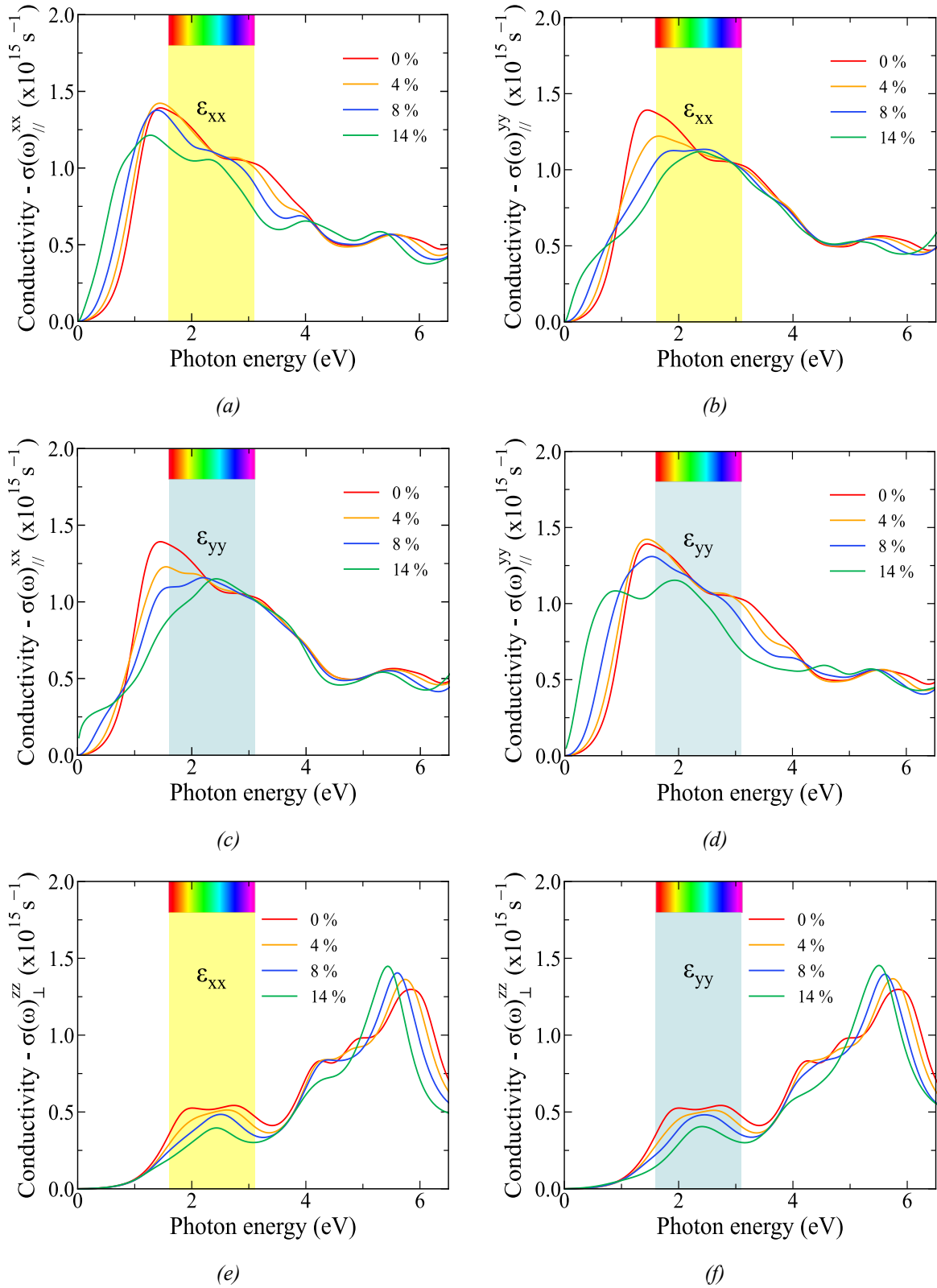


Fig. 7. The conductivity $\sigma(\omega)$ of monolayer NiS_2 : (a), (b) with the parallel polarized light under the x-direction tensile strain; (c), (d) and the parallel polarized light under the y-direction tensile strain; (e), the perpendicularly polarized light under tensile strain in the x-direction; (f) with the perpendicularly polarized light under the y-direction tensile strain.

3.4. Optical Conductivity

In this section, the optical properties of monolayer NiS₂ are investigated through the Density Function Theory (DFT) and the PBE functional. This study calculates the optical conductivity based on the below formula (3) [15]:

$$\sigma(\omega) = \frac{\omega}{4\pi} \cdot \epsilon_2(\omega) \quad (3)$$

where $\sigma(\omega)$ is the optical conductivity and $\epsilon_2(\omega)$ is the imaginary part based on the sum of the occupied-unoccupied transitions. Fig.7 illustrates the effects of tensile strain in the x and y directions on the optical conductivity $\sigma(\omega)$ of monolayer NiS₂, in the parallel (σ_{xx} , σ_{yy}) and perpendicular (σ_{\perp}) polarized regions. At the equilibrium state, the highest conductivities are $\sigma_{xx}^{\max} = 1.39 \times 10^{15} \text{s}^{-1}$ in the infrared light range (the light energy region $< 1.6 \text{eV}$) and $\sigma_{\perp}^{\max} = 1.45 \times 10^{15} \text{s}^{-1}$ in the ultraviolet region (the energy region $> 3.1 \text{eV}$). The obtained values of monolayer NiS₂ are similar to that of InTe [15].

In general, the distribution of optical conductivity depends on the mechanical strain. Under the tensile strain in the x and y directions, the conductivity $\sigma_{ij}(\omega)$ increases in the energy range from 0 eV to 1 eV, and decreases in the energy range $> 1 \text{eV}$, Fig. 7 (a, b, c, d). The conductivity $\sigma_{\perp}(\omega)$, which tends to decrease as the strain increases in the low-energy region ($< 5 \text{eV}$), and increases with strain in the higher energy region ($> 5 \text{eV}$), Fig. 7 (e, f). On the other hand, the result shows that the conductivities under the tensile strain in the x direction (Fig.7 (a, b)) are similar to that in the y direction, Fig.7 (c, d). We can see that, the highest value of the conductivity at the strain (ϵ_{xx}) 4% is $\sigma_{xx}^{\max} = \sigma_{yy}^{\max} = 1.42 \times 10^{15} \text{s}^{-1}$ increasing $\sim 2.2\%$ compared to that of the equilibrium state, and $\sigma_{xx}^{\max} = 1.21 \times 10^{15} \text{s}^{-1}$ at $\epsilon_{xx} = 14\%$ (decreasing $\sim 15\%$), Fig.7 (a, d). The conductivity $\sigma_{\perp}(\omega)$ under the tensile strain in the x and y directions has the same result and is the highest at $\sigma_{\perp}^{\max} = 1.45 \times 10^{15} \text{s}^{-1}$ for 5.43 eV (increasing 11,7% compared to the equilibrium state), Fig. 7 (e, f). Therefore, the conductivity of monolayer NiS₂ can be controlled by the strain.

4. Conclusion

To sum up, the properties of NiS₂ monolayer structure are investigated via the density functional theory (DFT). The NiS₂ expresses the critical strain at 18% in the x direction and 14% in the y direction with the ultimate strength of 8.0 N/m and 6.44N/m respectively. The NiS₂ structure with a band gap of 0.49 eV exhibits semiconductor properties with small carrier mobility. Under the mechanical strain, the carrier mobility of charged particles is significantly

improved (increasing 61.6 % in the x direction and 71.7 % in the y direction). The optical conductivity of the NiS₂ structure investigated has significant changes under the strain and becomes a potential candidate in fiber optic applications. Our results provide detailed information on the effect of the strain on the band gap, the carrier mobility, and the effective mass of charged particles in the NiS₂ structure. The mechanical strain is a useful parameter that enhances the properties of NiS₂ in nanoscale electronic and optical devices.

Reference

- [1] A. Shafique, A. Samad, and Y. H. Shin, Ultra low lattice thermal conductivity and high carrier mobility of monolayer SnS₂ and SnSe₂: A first principles study, *Phys. Chem. Chem. Phys.*, vol. 19, no. 31, 20677–20683, 2017.
[https://doi: 10.1039/c7cp03748a](https://doi.org/10.1039/c7cp03748a).
- [2] V. Van Thanh, D. Van Truong, and N. T. Hung, Charge-induced electromechanical actuation of two-dimensional hexagonal and pentagonal materials, *Phys. Chem. Chem. Phys.*, vol. 21, no. 40, 22377–22384, 2019.
[https://doi: 10.1039/c9cp03129d](https://doi.org/10.1039/c9cp03129d).
- [3] Q. Zhao, Y. Guo, K. Si, Z. Ren, J. Bai, and X. Xu, Elastic, electronic, and dielectric properties of bulk and monolayer ZrS₂, ZrSe₂, HfS₂, HfSe₂ from van der Waals density-functional theory, *Phys. Status Solidi Basic Res.*, vol. 254, no. 9, 2017.
[https://doi: 10.1002/pssb.201700033](https://doi.org/10.1002/pssb.201700033).
- [4] V. Van Thanh, N. D. Van, D. Van Truong, R. Saito, and N. T. Hung, First-principles study of mechanical, electronic and optical properties of Janus structure in transition metal dichalcogenides, *Appl. Surf. Sci.*, vol. 526, 146730–29, 2020.
[https://doi: 10.1016/j.apsusc.2020.146730](https://doi.org/10.1016/j.apsusc.2020.146730).
- [5] H. Khalatbari, S. I. Vishkayi, M. Oskouian, and H. R. Soleimani, Band structure engineering of NiS₂ monolayer by transition metal doping, *Sci. Rep.*, vol. 11, no. 1, 1–10, 2021.
[https://doi: 10.1038/s41598-021-84967-3](https://doi.org/10.1038/s41598-021-84967-3).
- [6] W. Xiong, K. Huang, and S. Yuan, The mechanical, electronic and optical properties of two-dimensional transition metal chalcogenides MX₂ and M₂X₃ (M = Ni, Pd; X = S, Se, Te) with hexagonal and orthorhombic structures, *J. Mater. Chem. C*, vol. 7, no. 43, 13518–13525, 2019.
[https://doi: 10.1039/c9tc04933a](https://doi.org/10.1039/c9tc04933a).
- [7] H. Yang *et al.*, First-principles calculations of the electronic properties of two-dimensional pentagonal structure XS₂ (X=Ni, Pd, Pt), *Vacuum*, vol. 174, no. January, 109176, 2020,
[https://doi: 10.1016/j.vacuum.2020.109176](https://doi.org/10.1016/j.vacuum.2020.109176).
- [8] P. J. and V. B. Shenoy, Tuning the Electronic Properties of Semi-conducting Transition Metal Dichalcogenides by Applying Mechanical Strains, *ACS Nano*, vol. 6, no. 6, 5449–5456, 2012.
[https://doi: 10.1021/nn301320r](https://doi.org/10.1021/nn301320r).
- [9] V. Van Thanh, N. D. Van, D. Van Truong, and N. T. Hung, Effects of strain and electric field on electronic

- and optical properties of monolayer γ -GeX (X = S, Se and Te), *Appl. Surf. Sci.*, vol. 582, no. January, 2022. [https://doi: 10.1016/j.apsusc.2021.152321](https://doi.org/10.1016/j.apsusc.2021.152321).
- [10] F. Mouhat and F. X. Coudert, Necessary and sufficient elastic stability conditions in various crystal systems, *Phys. Rev. B - Condens. Matter Mater. Phys.*, vol. 90, no. 22, 224104–4, Dec. 2014. [https://doi: 10.1103/PhysRevB.90.224104](https://doi.org/10.1103/PhysRevB.90.224104).
- [11] B. Mortazavi, O. Rahaman, M. Makaremi, A. Dianat, G. Cuniberti, and T. Rabczuk, First-principles investigation of mechanical properties of silicene, germanene and stanene, *Phys. E Low-Dimensional Syst. Nanostructures*, vol. 87, 228–232, 2017. [https://doi: 10.1016/j.physe.2016.10.047](https://doi.org/10.1016/j.physe.2016.10.047).
- [12] P. Miró, M. Ghorbani-Asl, and T. Heine, Two dimensional materials beyond MoS₂: Noble-transition-metal dichalcogenides, *Angew. Chemie - Int. Ed.*, vol. 53, no. 11, 3015–3018, 2014. [https://doi: 10.1002/anie.201309280](https://doi.org/10.1002/anie.201309280).
- [13] T. V. Vu, H. V. Phuc, C. V. Nguyen, A. I. Kartamyshev, and N. N. Hieu, A theoretical study on elastic, electronic, transport, optical and thermoelectric properties of Janus SnSO monolayer, *J. Phys. D. Appl. Phys.*, vol. 54, no. 47, 2021. [https://doi: 10.1088/1361-6463/ac1d73](https://doi.org/10.1088/1361-6463/ac1d73).
- [14] H. V. Phuc *et al.*, Tuning the electronic properties, effective mass and carrier mobility of MoS₂ monolayer by strain engineering: First-principle calculations, *J. Electron. Mater.*, vol. 47, no. 1, 730–736, 2017. [https://doi: 10.1007/s11664-017-5843-8](https://doi.org/10.1007/s11664-017-5843-8).
- [15] T. N. Do, V. T. T. Vi, N. T. T. Binh, N. N. Hieu, and N. V. Hieu, Computational study on strain and electric field tunable electronic and optical properties of InTe monolayer, *Superlattices Microstruct.*, vol. 151, no. January, 2021, [https://doi: 10.1016/j.spmi.2021.106816](https://doi.org/10.1016/j.spmi.2021.106816).